

New approaches to the synthesis of selected hydroxyquinolines and their hydroxyquinoline carboxylic acid analogues

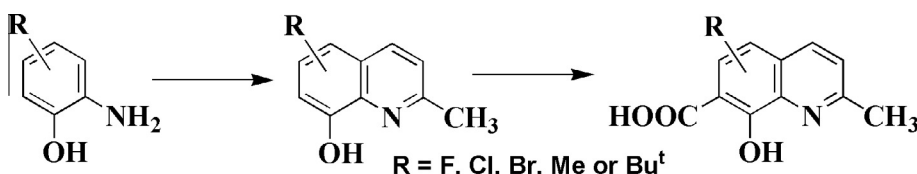
Marcin Szala, Jacek E. Nycz*, Grzegorz J. Malecki

Institute of Chemistry, University of Silesia, ul. Szkolna 9, PL-40007 Katowice, Poland

HIGHLIGHTS

- Three hydroxyquinolines have been characterized by X-ray diffraction method.
- The X-ray structure of 5-chloro-8-hydroxy-2-methylquinoline-7-carboxylic acid.
- New approaches to the Skraup synthesis of selected hydroxyquinolines.

GRAPHICAL ABSTRACT



ARTICLE INFO

Article history:

Received 17 February 2014
 Received in revised form 24 March 2014
 Accepted 16 April 2014
 Available online xxxx

Keywords:

Quinoline
 Carboxylic acid
 Hydroxyquinoline
 Hydroxyquinoline carboxylic acid
 Skraup
 Substituent effect

ABSTRACT

New approaches to the synthesis of selected crystalline hydroxyquinolines and their carboxylic acid analogues were elaborated in this paper with the auxiliary of computational and spectroscopic characterization, such as FTIR, NMR and single crystal X-ray measurements. The experimental data were further rationalized based on a DFT calculation method with B3LYP functional, which reflected the impact of electron donating or withdrawing groups on the energy level of HOMO orbitals and the reactivity of the substituted hydroxyquinolines.

© 2014 Elsevier B.V. All rights reserved.

Introduction

Quinolines were first discovered from coal tar by Friedlieb Ferdinand Runge in 1834 [1]. After half century Skraup–Doebner–Miller successfully synthesized the quinolines in laboratory [2–5]. For 180 years many synthetic protocols and applications have been developed based on the Skraup transformation because of its simplicity and the importance of the quinoline itself [6–18].

We are particularly interested in the functionalization of benzene (or phenol) ring in quinoline (or hydroxyquinoline) constitution from both theoretical and practical point view. Recently derivatives of quinoline with both hydroxyl and carboxylic acid

groups on benzene ring have attracted increased attention due to their analogy to the precursor of a promising HIV-1 integrase inhibitor, 2-[(E)-2-(3,4-dihydroxy-5-methoxyphenyl)ethenyl]-8-hydroxyquinoline-7-carboxylic acid (FZ-41) which has been demonstrated to block the replication of HIV-1 in cell cultures at nontoxic concentrations [19,20]. The modifications of quinoline moiety through introducing carboxylic acid function increased their acidity and water solubility. In consequence this could increase their bioavailability and biological activity, and could trigger searches on new biological applications of the compounds.

In this paper, we reported new approaches to the synthesis of the aforementioned compounds with in-depth spectroscopic characterization. Computational and spectroscopic studies were carried out to compare selected hydroxyquinolines and hydroxyquinoline carboxylic acid, which have not been reported by previous studies according to our best knowledge.

* Corresponding author. Tel.: +48 32 359 1206; fax: +48 32 259 9978.

E-mail address: jnycz@us.edu.pl (J.E. Nycz).

Experimental

General

NMR spectra were obtained with Bruker Avance 400 and 500 operating at 400.13 MHz (^1H) and 100.5 MHz (^{13}C) at 21 °C; chemical shifts referenced to ext. TMS (^1H , ^{13}C); coupling constants are given in Hz. The ^1H and ^{13}C NMR calculations were performed with the ACD Labs NMR Predictor v.8 program. For GC/MS, a Gas Chromatograph TRACE 2000 with MS Finnigan TRACE (ThermoQuest) with autosampler Combi PAL (CTC) with capillary column DB-5 MS 30 m \times 0.25 μm \times 0.5 μm was used. Mass spectra were obtained with a Varian 500 MS with applied ESI technique. FTIR spectra were recorded on a Perkin Elmer spectrophotometer in the spectral range 4000–450 cm^{-1} with the samples in the form of KBr pellets. Electronic spectra were measured on a spectrophotometer Lab. Chromatography was carried out on Silica Gel 60 (0.15–0.3 mm) Machery Nagel. Melting points were determined on MPA100 OptiMelt melting point apparatus and uncorrected. 2-Amino-4-*tert*-butylphenol (**1a**), 2-amino-5-methylphenol (**1b**), 2-amino-4-bromophenol (**1c**), 2-amino-4-chlorophenol (**1d**) and 2-amino-4-fluorophenol (**1e**) were purchased from Sigma–Aldrich, and were used without further purification.

The synthesis of quinolines **2a**, **2b**, **2c**, **3a**, **3b** and **3c** followed our procedure described in the literature [6,7]:

5-*tert*Butyl-2-methyl-quinolin-8-ol (**2a**)

16%; mp = 54.5 °C; IR (KBr; cm^{-1}): 3344 ν_{OH} ; 2994, 2955, 2913, 2874 $\nu_{\text{CH}_3, \text{t-Bu}}$; 1576 $\nu_{\text{C}=\text{N}}$; ^1H NMR (CDCl_3 ; 500.18 MHz) δ = 1.55 (s, 9H, Bu^t), 2.72 (s, 3H, CH₃), 7.05 (d, J = 8.1 Hz, 1H, aromatic), 7.30 (d, J = 8.9 Hz, 1H, aromatic), 7.37 (d, J = 8.1 Hz, 1H, aromatic), 8.66 (d, J = 8.9 Hz, 1H, aromatic); $^{13}\text{C}\{^1\text{H}\}$ NMR (CDCl_3 ; 125.78 MHz) δ = 24.51, 32.08, 35.55, 108.78, 121.11, 123.53, 124.92, 135.83, 136.59, 138.83, 150.16, 155.32; t_r = 6.98 min, GC/MS: (EI) M^+ = 215 (65%), ($M+H$)⁺ = 216 (10%), ($M-\text{CH}_3$)⁺ = 200 (100%); CCDC 963546.

2,6-Dimethylquinolin-8-ol (**2b**)

26%; mp = 136.6 °C; IR (KBr; cm^{-1}): 3347 ν_{OH} ; 2916, 2849 ν_{CH_3} ; 1570 $\nu_{\text{C}=\text{N}}$; ^1H NMR (CDCl_3 ; 500.18 MHz) δ = 2.47 (s, 3H, CH₃), 2.70 (s, 3H, CH₃), 7.01 (d, J = 1.3 Hz, 1H, aromatic), 7.05 (bs, 1H, aromatic), 7.24 (d, J = 8.4 Hz, 1H, aromatic), 7.93 (d, J = 8.4 Hz, 1H, aromatic); $^{13}\text{C}\{^1\text{H}\}$ NMR (CDCl_3 ; 125.78 MHz) δ = 22.19, 24.79, 112.17, 116.78, 122.83, 126.71, 135.78, 136.21, 137.02, 151.31, 155.93; t_r = 12.01 min, GC/MS: (EI) M^+ = 173 (100%), ($M+H$)⁺ = 174 (12%); CCDC 973848.

5-Bromo-2-methylquinolin-8-ol (**2c**)

34%; mp = 66.1 °C (lit. 69 °C [32]); IR (KBr; cm^{-1}): 3373 ν_{OH} ; 2920, 2874 ν_{CH_3} ; 1595 $\nu_{\text{C}=\text{N}}$; 1500, 1256; (IR (KBr): 3375, 1500, 1390, 1255 cm^{-1} [32]); ^1H NMR (CDCl_3 ; 500.18 MHz) δ = 2.78 (s, 3H, CH₃), 7.05 (d, J = 8.2 Hz, 1H, aromatic), 7.42 (d, J = 8.6 Hz, 1H, aromatic), 7.64 (d, J = 8.2 Hz, 1H, aromatic), 8.38 (d, J = 8.6 Hz, 1H, aromatic) (lit. ^1H NMR (CDCl_3) δ = 2.73 (s, 3H), 7.01 (d, J = 8.2 Hz, 1H), 7.38 (d, J = 8.6 Hz, 1H), 7.60 (d, J = 8.2 Hz, 1H), 8.31 (d, J = 8.6 Hz, 1H) [32]); $^{13}\text{C}\{^1\text{H}\}$ NMR (CDCl_3 ; 125.78 MHz) δ = 24.76, 109.77, 110.76, 123.92, 126.00, 130.14, 136.04, 138.46, 151.71, 157.80 (^{13}C NMR (CDCl_3) δ = 24.7, 109.6, 110.5, 123.8, 125.7, 129.9, 135.7, 138.3, 151.5, 157.6 [32]); t_r = 6.82 min, GC/MS: (EI) M^+ = 237 (100%), 239 (96%), ($M+H$)⁺ = 238 (15%), 240 (14%).

5-Chloro-8-hydroxy-2-methylquinoline-7-carboxylic acid (**3a**)

43%; IR (KBr; cm^{-1}): 3355 ν_{OH} ; 2919 ν_{CH_3} ; 1597 $\nu_{\text{as}(\text{COO})}$; 1570 $\nu_{\text{C}=\text{N}}$; 1330 $\nu_{\text{s}(\text{COO})}$; CCDC 969571.

5-Bromo-8-hydroxy-2-methylquinoline-7-carboxylic acid (**3b**)

<1%; mp_{dec.} = 214.2 °C; IR (KBr; cm^{-1}): 3416 ν_{OH} ; 2831 ν_{CH_3} ; 1598 $\nu_{\text{as}(\text{COO})}$; 1363 $\nu_{\text{s}(\text{COO})}$; ^1H NMR (KOD/D₂O/DMSO-*d*₆; 500.18 MHz) δ = 2.91 (s, 3H, CH₃), 6.89 (d, J = 8.4 Hz, 1H, aromatic), 7.71 (d, J = 8.5 Hz, 1H, aromatic), 8.20 (s, 1H, aromatic); MS: (ESI) (DMSO) ($M-H+Na$)⁺ = 302 (100%), 304 (96%).

The isolated yield of acids **3a** and **3c** have been improved:

5-Fluoro-8-hydroxy-2-methylquinoline-7-carboxylic acid (**3c**) 70% [6].

Crystallization

The crystals suitable for X-ray analysis were obtained from hexane solution at room temperature for **2a**, **2b** and from AcOEt solution for **3a**.

DFT calculations

The calculations were carried out by using Gaussian09 program [21]. Molecular geometries of the singlet ground state of compounds **2a**, **2b** and **3a** were fully optimized in the gas phase at the B3LYP level of theory [22,23]. For each compound a frequency calculation was carried out, verifying that the optimized molecular structure obtained corresponded to an energy minimum, thus only positive frequencies were expected. The calculations were performed using the 6-31G** functions for all atoms.

Crystal structure determination and refinement

The crystals of the compounds were mounted in turn on a Gemini A ultra Oxford Diffraction automatic diffractometer equipped with a CCD detector for data collection. X-ray intensity data were collected with graphite monochromated Mo K α radiation (λ = 0.71073 Å) at temperature of 295(2) K, with ω scan mode. Ewald sphere reflections were collected up to 2θ = 50.10. Lorentz, polarization and empirical absorption correction using spherical harmonics implemented in SCALE3 ABSPACK scaling algorithm were applied [24]. The structures were solved by the direct method and subsequently completed by the difference of Fourier recycling. All the non-hydrogen atoms were refined anisotropically using a full-matrix least-squares technique. The Olex2 and SHELXS, SHELXL programs were used for all the calculations [25,26]. Atomic scattering factors were incorporated in the computer programs. Details of crystal data and refinement are gathered in Table 1.

Results and discussion

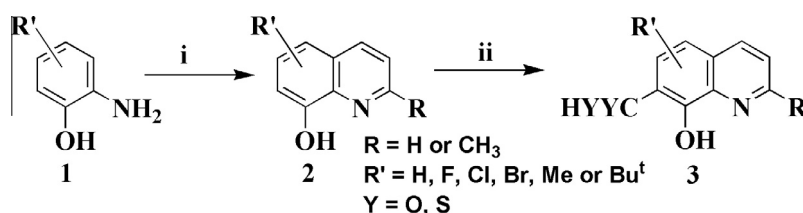
In our previous and present studies, the synthesis of some hydroxyquinolines and their carboxylic acid derivatives have been reported and characterized by using IR, MS, UV–Vis, multinuclear NMR spectroscopic techniques, and single crystal X-ray diffraction method (Scheme 1) [6,7]. X-ray crystal structure analysis showed the presence of hydrogen-bond donating and accepting sites between the pyridine and hydroxyl functional groups. It has been demonstrated by solution and solid state NMR studies that there was a tautomeric equilibrium among the neutral, cationic and anionic species of hydroxyquinoline carboxylic acids obtained by protonation or deprotonation, through the evaluation of ^{13}C and ^{15}N chemical shifts [10]. The largest effect is visible in the ^{15}N NMR spectra which allow to distinguish the species between protonated and unprotonated pyridine rings. These measurements are best applicable in the solid state.

Synthetic remarks

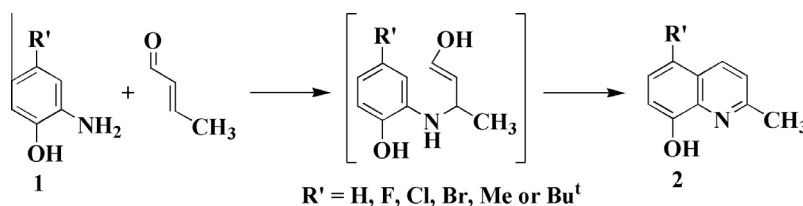
The compounds of hydroxymethylquinolines **2a**, **2b** and **2c** have been synthesized by adopting Skraup–Doebner–Von Miller

Table 1
Crystal data and structure refinement details of **2a**, **2b** and **3a**.

	2a	2b	3a
Empirical formula	C ₁₄ H ₁₇ NO	C ₁₁ H ₁₁ NO	C ₁₁ H ₈ ClNO ₃ , H ₂ O
Formula weight	215.29	173.21	255.66
Temperature (K)	295.0(2) K	295.0(2) K	295.0(2) K
Crystal system	Orthorhombic	Orthorhombic	Monoclinic
Space group	Pnma	P2 ₁ 2 ₁ 2 ₁	P2 ₁ /n
Unit cell dimensions			
<i>a</i> (Å)	16.9534(15)	6.5547(6)	9.5478(7)
<i>b</i> (Å)	7.1811(7)	11.4741(13)	24.642(2)
<i>c</i> (Å)	9.8632(10)	11.7144(12)	10.0327(7)
α (°)	90	90	90
β (°)	90	90	112.716(8)
γ (°)	90	90	90
Volume (Å ³)	1200.8(2)	881.03(16)	2177.4(3)
<i>Z</i>	4	4	8
Calculated density (Mg/m ³)	1.191	1.306	1.560
Absorption coefficient (mm ⁻¹)	0.075	0.084	0.353
<i>F</i> (000)	464	368	1056
Crystal dimensions (mm)	0.34 × 0.32 × 0.21	0.38 × 0.11 × 0.09	0.23 × 0.14 × 0.03
θ range for data collection (°)	3.51–25.05	3.48–25.05	3.39–25.05
Index ranges	–20 ≤ <i>h</i> ≤ 20 –8 ≤ <i>k</i> ≤ 7 –10 ≤ <i>l</i> ≤ 11	–7 ≤ <i>h</i> ≤ 7 –13 ≤ <i>k</i> ≤ 13 –11 ≤ <i>l</i> ≤ 13	–10 ≤ <i>h</i> ≤ 11 –26 ≤ <i>k</i> ≤ 29 –11 ≤ <i>l</i> ≤ 10
Reflections collected	3768	4592	8805
Independent reflections	1153 [R _(int) = 0.0292]	1544 [R _(int) = 0.0340]	3836 [R _(int) = 0.0633]
Data/restraints/parameters	1153/0/97	1544/0/121	3836/0/317
Flack parameter		0.01(2)	
Goodness-of-fit on <i>F</i> ²	1.098	1.065	0.993
Final <i>R</i> indices [<i>I</i> > 2σ(<i>I</i>)]	<i>R</i> ₁ = 0.0501 <i>wR</i> ₂ = 0.1195	<i>R</i> ₁ = 0.0410 <i>wR</i> ₂ = 0.1001	<i>R</i> ₁ = 0.0607 <i>wR</i> ₂ = 0.1547
<i>R</i> indices (all data)	<i>R</i> ₁ = 0.0779 <i>wR</i> ₂ = 0.1336	<i>R</i> ₁ = 0.0508 <i>wR</i> ₂ = 0.1072	<i>R</i> ₁ = 0.0899 <i>wR</i> ₂ = 0.1872
Largest diff. Peak and hole	0.287 and –0.420	0.126 and –0.159	0.528 and –0.454
CCDC number	963546	973848	969571



Scheme 1. Synthesis of hydroxyquinolines and their carboxylic acid analogues. Reagents and conditions: i; CH₃CHCHCHO, 6 M HCl, reflux; ii; Bu^tOK, THF 20 °C; CO₂ or CS₂.



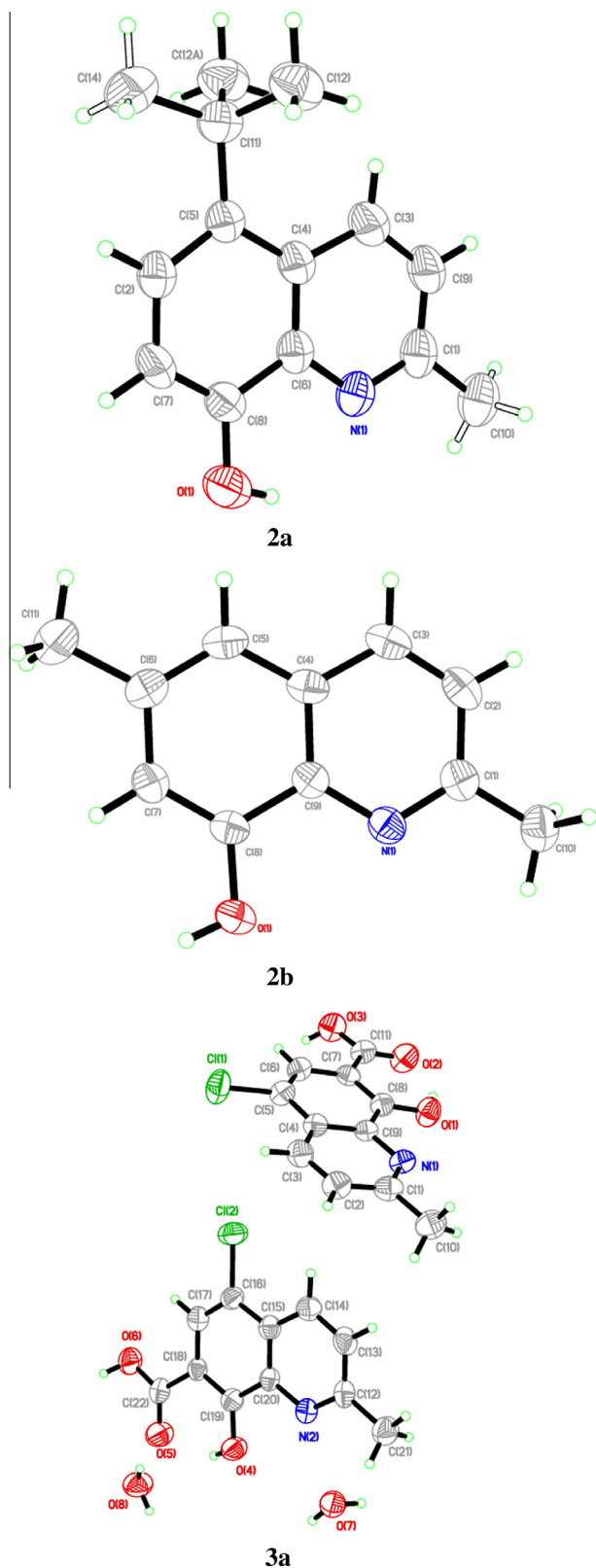
Scheme 2. Synthesis of hydroxyquinolines. Proposed mechanism.

reaction, with modified Matsugi two-phase solvent system [27]. The presented results are the continuation of our recent papers [6,7]. In order to obtain a better understanding of Skraup transformation, another aniline type reagents were chosen, which possessed substituents with varying volumes located at different positions on benzene ring (Schemes 1 and 2).

Interestingly it has been noticed that bulky substituents such as *tert*-butyl in the case of **2a** led to decreased productivity comparing with methyl group **2b** or bromine for **2c** and previously reported results (Scheme 1 and 2) [6,7]. A plausible explanation for the

observation is that it is relevant to a ring closure reaction to create pyridine ring followed by oxidation to the final quinoline (Scheme 2). Considering the previous and present studies, it is deduced that the pattern of the yield distribution and regioselectivity depend on the substituent volumes, electronic factors and possible internal hydrogen bonds for intermediate (Scheme 2).

Presented here **3a**, **3b** and **3c** have been synthesized by adopting Kolbe–Schmidt reaction with some modification reported in our previous studies [6,7]. The isolated yield of acids **3a** and **3c** have been improved.

**Table 2**Selected bond lengths and angles for compound **2a**, **2b** and **3a** with hydrogen bonds (Å and °).

	2a	2b	3a^a	
C(8)–O(1)	1.362(3)	1.353(2)	1.324(4)	
C(1)–N(1)	1.322(3)	1.330(2)	1.318(4)	
C(9)–N(1)	1.362(3)	1.379(2)	1.375(4)	
C(1)–C(10)	1.500(4)	1.492(3)	1.503(5)	
C(5/6/7)–C(11)	1.533(3)	1.508(3)	1.497(5)	
C(5)–Cl(1)			1.740(4)	
C(11)–O(2)			1.233(4)	
C(11)–O(3)			1.273(4)	
C(1)–N(1)–C(9)	118.8(2)	118.11(16)	118.2(3)	
N(1)–C(1)–C(2)	120.6(2)	121.81(18)	122.4(3)	
N(1)–C(1)–C(10)	117.5(2)	118.11(18)	116.4(4)	
C(7)–C(8)–O(1)	122.0(2)	123.47(17)	124.2(3)	
C(5)–C(11)–C(12)	110.56(14)	123.20(6)		
C(14)–C(11)–C(5)	111.9(2)			
C(5)–C(6)–C(11)		121.53(19)		
C(6)–C(7)–C(11)			120.2(3)	
C(4)–C(5)–Cl(1)			119.1(3)	
O(2)–C(11)–O(3)			124.2(3)	
D–H...A	d (D–H)	d (H...A)	d (D...A)	<(DHA)
2a				
O(1)–H(1)...N(1)	0.81	2.16	2.626(3)	116.9
2b				
O(1)–H(1)...N(1) ^b	0.82	2.08	2.838(2)	153.8
3a				
O(1)–H(1)...O(2)	0.82	1.83	2.549(3)	145.3
O(4)–H(4)...O(5)	0.82	1.84	2.548(3)	143.2
C(3)–H(3A)...Cl(1)	0.93	2.70	3.077(4)	104.9
C(14)–H(14)...Cl(2)	0.93	2.69	3.070(4)	105.5

^a Average values.^b Symmetry transformation used to generate equivalent atoms: 1/2 + x, 3/2 – y, –z.

markedly shifted to downfield (larger δ ; deshielding effect), similarly to our previous results [6,7]. On the contrary the CH₃ protons on phenol ring were shifted to upfield (smaller δ ; the shielding effect). The experimental and the calculated data are in good agreement (Tables S1 and S2). ACD/Labs NMR predictors can be trained with experimental data to improve NMR prediction accuracy of compounds which were not described in publications or DB.

X-ray and DFT studies

Compounds **2a** and **2b** belong to the orthorhombic *Pnma* or *P2₁2₁2₁* space groups while compound **3a** crystallized as hydrate in the monoclinic *P2₁/n* space group. The asymmetric unit of **3a** is composed from two independent molecules. The crystal structures of the compounds are shown, as ORTEP representation, in Fig. 1. Selected bond lengths and angles are collected in Table 2.

The quinoline rings are planar within experimental error and the C(1)–N(1) distances, similar in the compounds, in the range from 1.318(4) Å to 1.322(3) Å, which clearly indicate they are double bonds. The C(8)–O(1) distance in the **3a** is shorten by about 0.03 Å than in **2b** which is connected with electron withdrawing effect exerted by chloride in position 5 in the quinoline ring. In the case of **2a** the distance is slightly longer than in **2b** due to the effect of electron releasing *tert*-butyl group. The angles in the quinoline rings do not show any particular deviations from the value of 120°. In these molecules, the observed intra- and intermolecular short contact (Table 2) according to Desiraju and Steiner, can be classified as weak hydrogen bond [28]. Moreover in the structure of **2b** the hydrogen bonds form infinite intermolecular chain of C₁(5)*a* type. In the structure of **3a**, intra- and intermolecular motifs are observed, which belong to discrete chains with degrees from 2 to 8 (*D*₁¹(2); *D*₂²(4); *D*₂²(5); *D*₂²(6); *D*₂²(8)) and self-rings created by interaction between carboxyl groups, water molecules and hydroxyl group (*S*₁¹(6)). Moreover, the structure of **3a** is stabilized by

Fig. 1. ORTEP drawings of **2a**, **2b** and **3a** molecules with 50% probability displacement ellipsoids.

The ¹H NMR spectra of hydroxyquinolines showed distinctive H-1 signals from CH₃ group (Table S1). The analysis of the trend in ¹H chemical shifts revealed that protons of methyl group located at 2 position of pyridine ring in quinoline constitution were

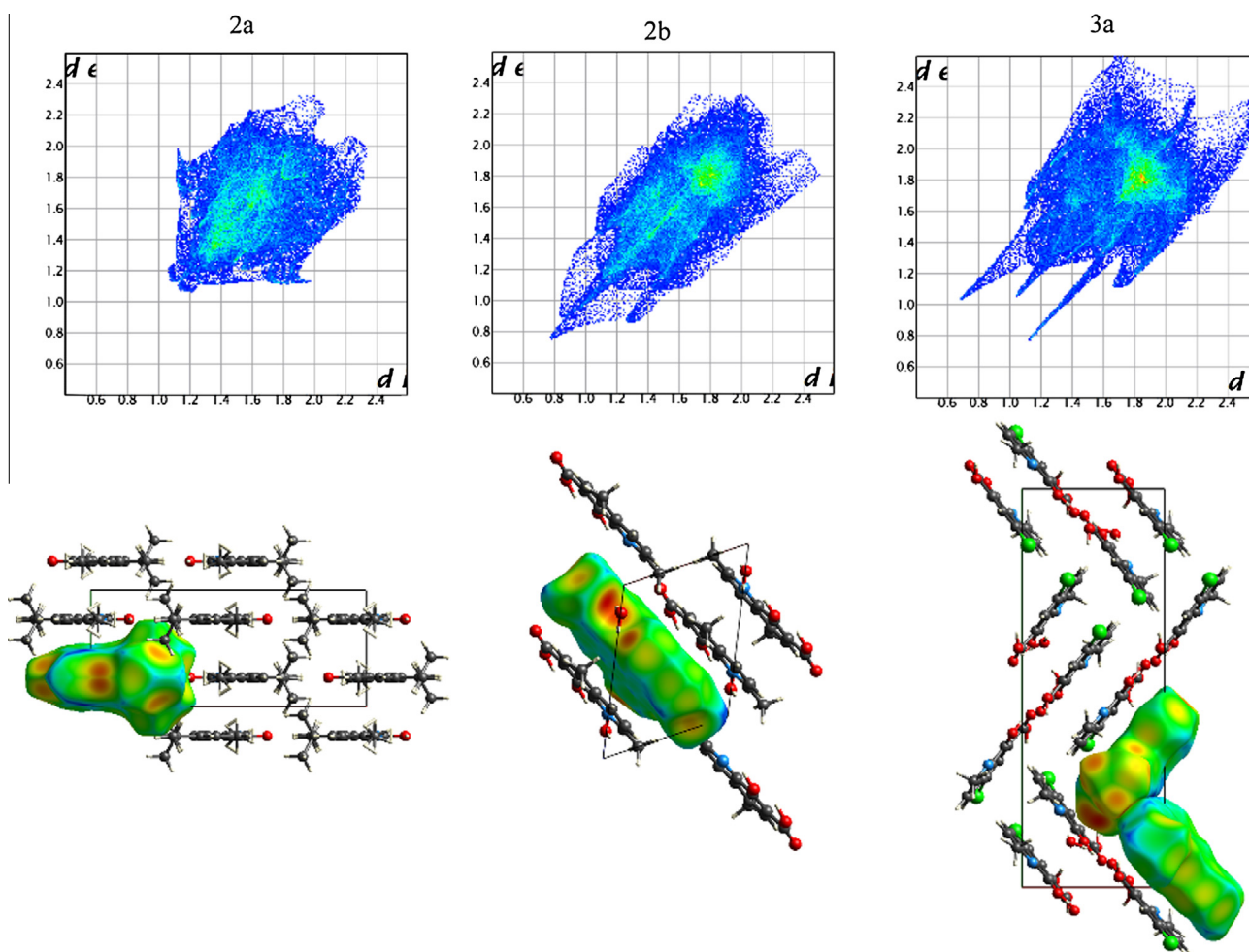


Fig. 2. 2D fingerprint plots with Hirshfeld surfaces and packing of molecules in the crystal lattices of **2a**, **2b** and **3a** compounds.

some electronic interactions detailed in Table 2. The molecular arrangements in **2a**, **2b** and **3a** were analyzed by means of the Hirshfeld surfaces and of the corresponding 2D-fingerprint-plots generated by CrystalExplorer program [29–31]. The 2D-fingerprint plots are presented in Fig. 2 and the percentage contributions to the Hirshfeld surface area for the various close intermolecular contacts for the molecules given on the histogram for the major atom-type/atom-type contacts are presented in Fig. 3.

The fingerprint plots show that the compounds share some similar structural features as the hydrogen bonds $O\cdots H$ and $H\cdots H$ contacts in the limit of the van der Waals radii. The hydrogen bond dominates the shape of all plots, appearing as a pair of sharp spikes at the bottom left of the plot (the upper one associated with the donor atom and the lower one with the acceptor). A difference between the molecular interactions in **2a**, **2b** and **3a** in terms of $N\cdots H/O\cdots H$ interactions is reflected in the length of spikes. The trace in the fingerprint of **2a** reflects the longer bond than in the **2b**. Similarly the lengths of the spikes in the fingerprint of **2b** molecule correlate with the intermolecular chain formed by hydrogen bonds. The wings on the plot of **3a** demonstrate the diversity of the hydrogen bonds, such as $O\cdots H\cdots O$ and $CH\cdots Cl$ (see Table 2). Another type of $C\cdots H\cdots \pi$ interaction in **3a** also contributes to the wings in the plots of the molecule. Moreover in the 2D plot, the red region in distance about 3.6 Å indicates the existence of π -stacking interaction between phenyl rings in the structure of **3a**. The interaction of $C\cdots H\cdots \pi$ and $\pi\cdots\pi$ stacking are collected in Table 3. The intermolecular $H\cdots H$ contacts in the range of the van

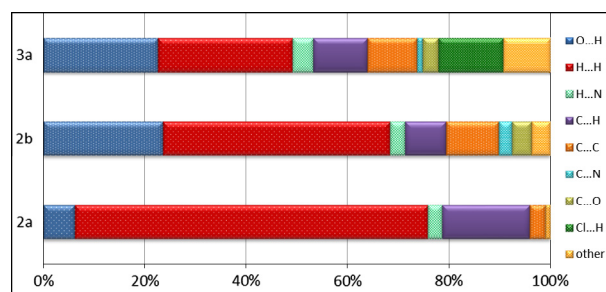


Fig. 3. Percentage contributions to the Hirshfeld surface area for the various close intermolecular contacts for the **2a**, **2b** and **3a** molecules.

der Waals radii show up as a characteristic hump in the central region of the plots, and in compound **2a** (Fig. 2) the contact also plays a significant role. The predominant role of these interactions is clearly visible from the histogram presented in Fig. 3. Whereas the $O\cdots H$ and $N\cdots H$ contacts contributed in the structure of **2b** and **3a** showed much less impact in **2a**.

The geometry of **2a**, **2b** and **3a** (without the solvent molecule) were optimized in singlet states using the DFT method with the B3LYP functional. In general, the predicted bond lengths and angles are over-estimated by about 0.1 Å and 5° respectively (see Table S3 in supplementary materials). In addition, the calculated and experimental IR spectra show rather good compatibility as one can see from the data collected in Supplementary materials Table S4. The

Table 3
Electronic stacking interactions in molecular structure of **3a**.

	Angle (°)	Distance (Å)	Shift distance (Å)
Centroids: #Cg1: (C4–C9); #Cg2: (C15–C20); #Cg3: (N1, C1–C9); #Cg4: (N2, C12–C20)			
#Cg1 :#Cg2 ($-1/2 + x, 1/2 - y, -1/2 + z$)	3.347	3.734	1.687
#Cg1 :#Cg4 ($-1/2 + x, 1/2 - y, -1/2 + z$)	4.771	3.673	1.376
#Cg3 :#Cg4 ($-1/2 + x, 1/2 - y, -1/2 + z$)	5.152	3.825	1.758
#Cg2 :#Cg2 ($2 - x, -y, 2 - z$)	0.000	3.629	1.186

frontier orbitals are of extreme importance for the evaluation of molecular reactivity. As much is negative the energy of the Highest Occupied Molecular Orbital (HOMO), more susceptible is the molecule to donate electrons and, consequently, higher is the tendency to be oxidized. The similar principle can be used to interpret the tendency of a given molecule undergoing reduction, based on the energy of the Lowest Unoccupied Molecular Orbital (LUMO). The

contours of HOMOs and LUMOs are presented in Fig. 4. In general, for all these molecules, the HOMO orbitals are mainly concentrated in the phenyl ring, hydroxyl and chlorine.

The atomic charge calculations for **3a** show that chlorine substituents have charges close to zero (-0.044) similarly to our previous results [6,7,14,33]. The HOMO energies decrease in the order of **2a** > **2b** > **3a**, and this can be explained by the fact that a *tert*-butyl substituent in position 5 in quinoline ring exerts activating (electron donating group) effect which leads to a rise in HOMO energy (Fig. 4). On the other hand, chlorine in compound **3a** as an electron withdrawing group disturbs charge density and lowers the energy of HOMO.

Conclusions

The presented research has been focused on better understanding Skraup synthesis of hydroxyquinolines. Interestingly, we noticed that bulky substituents such as *tert*-butyl decreased the reaction productivity comparing with smaller group, such as

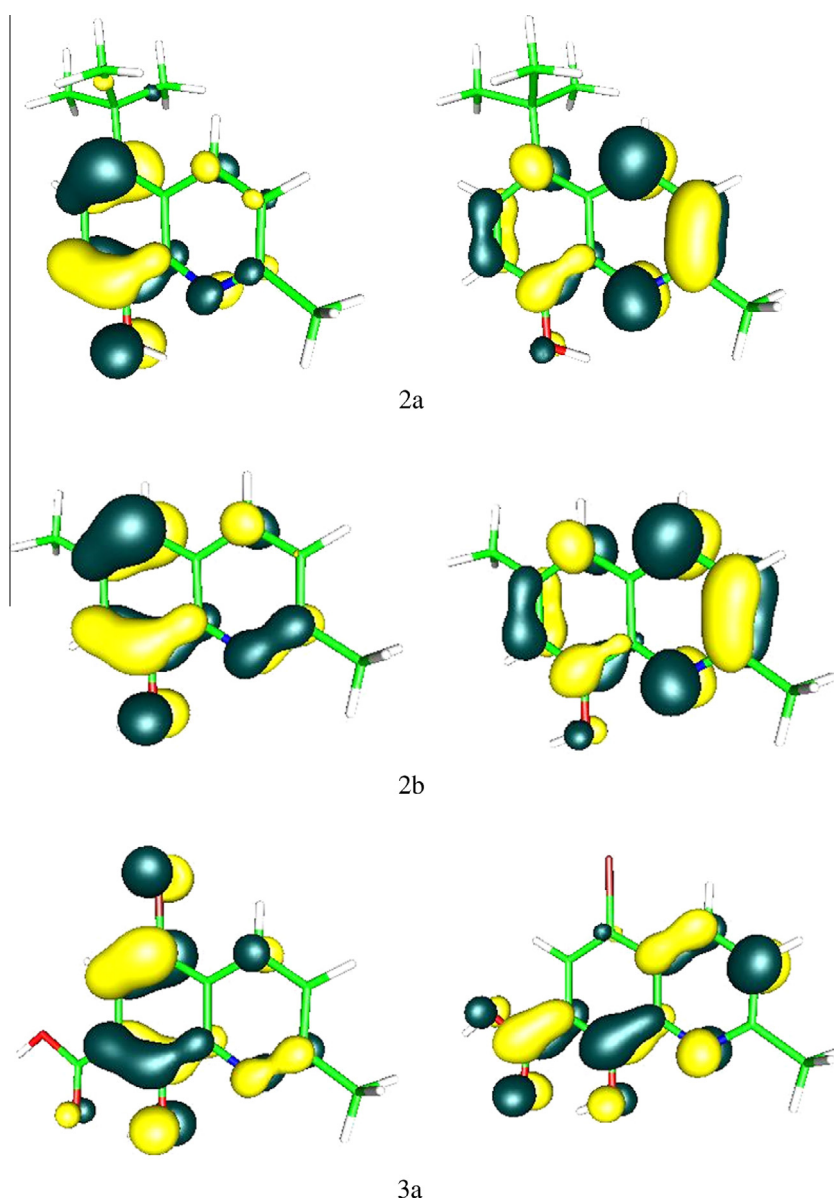


Fig. 4. Contours of HOMO, LUMO of the molecules **2a**, **2b** and **3a**.

methyl. A plausible explanation for the observed phenomenon might be due to the ring closure reaction to create pyridine ring in quinoline constitution, followed by oxidation to the final compound.

Acknowledgments

The GAUSSIAN09 calculations were carried out in the Wrocław Centre for Networking and Supercomputing, WCSS, Wrocław, Poland (<http://www.wcss.wroc.pl> grant number 18).

Appendix A. Supplementary material

CCDC 963546 for **2a**, CCDC 973848 for **2b** and CCDC 969571 for **3a** contains the supplementary crystallographic data for the compound. These data can be obtained free of charge from <http://www.ccdc.cam.ac.uk/conts/retrieving.html>, or from the Cambridge Crystallographic Data Centre, 12 Union Road, Cambridge CB2 1EZ, UK; fax: +44 1223 336 033; or e-mail: deposit@ccdc.cam.ac.uk. Calculations have been carried out in Wrocław Centre for Networking and Supercomputing (<http://www.wcss.wroc.pl>). Supplementary data associated with this article can be found, in the online version, at <http://dx.doi.org/10.1016/j.molstruc.2014.04.052>.

References

- [1] F. Runge, *Pogg. Ann. (Annalen der Phys. Chem.)* 31 (1834) 65–80.
- [2] Z.H. Skraup, *Monatsh Chem.* 1 (1880) 316–318.
- [3] Z.H. Skraup, *Monatsh Chem.* 2 (1881) 139–170.
- [4] Z.H. Skraup, *Monatsh Chem.* 2 (1881) 587–609.
- [5] Z.H. Skraup, *Ber Chem.* 15 (1882) 897.
- [6] J.E. Nycz, M. Szala, G.J. Malecki, M. Nowak, J. Kusz, *Spectrochim. Acta A* 117 (2014) 351–359.
- [7] J.E. Nycz, G.J. Malecki, *J. Mol. Struct.* 1032 (2013) 159–168.
- [8] J. Chojnacki, P. Skop, A. Pladzyk, J.E. Nycz, *Acta Cryst. E* 63 (2007) o4773–o4774.
- [9] B. Machura, J. Miłek, J. Kusz, J. Nycz, D. Tabak, *Polyhedron* 27 (2008) 1121–1130.
- [10] D. Gudat, J.E. Nycz, J. Polanski, *Magn. Reson. Chem.* 46 (2008) S115–S119.
- [11] L. Ponikiewski, J.E. Nycz, *Acta Cryst. E* 65 (2009) o515–o530.
- [12] J.E. Nycz, *Polish J. Chem.* 83 (2009) 1637–1642.
- [13] R. Musiol, J. Jampilek, J.E. Nycz, M. Pesko, J. Carroll, K. Kralova, M. Vejsova, J. O'Mahony, A. Coffey, A. Mrozek, J. Polanski, *Molecules* 15 (2010) 288–304.
- [14] G. Malecki, J.E. Nycz, E. Ryrzych, L. Ponikiewski, M. Nowak, J. Kusz, J. Pikies, *J. Mol. Struct.* 969 (2010) 130–138.
- [15] J.E. Nycz, G. Malecki, L. Ponikiewski, M. Leboschka, M. Nowak, J. Kusz, *J. Mol. Struct.* 986 (2011) 39–48.
- [16] A. Paretzki, H.S. Das, F. Weisser, T. Scherer, D. Dubrin, J. Fiedler, J.E. Nycz, B. Sarkar, *Euro. J. Inorg. Chem.* (2011) 2413–2421.
- [17] J.E. Nycz, G. Malecki, S. Chikkali, I. Hajdok, P. Singh, *Relat. Elem.* 187 (2012) 564–572.
- [18] W. Cieslik, R. Musiol, J.E. Nycz, J. Jampilek, M. Vejsova, M. Wolff, B. Machura, *J. Polanski, Bioorg. Med. Chem.* 20 (2012) 6960–6968.
- [19] F. Zouhiri, J.-F. Mouscadet, K. Mekouar, D. Desmaele, D. Savoure, H. Leh. F. Subra, M. Le Bret, C. Auclair, J. d'Angelo, *J. Med. Chem.* 43 (2000) 1533–1540.
- [20] S. Hare, A.M. Vos, R.F. Clayton, J.W. Thuring, M.D. Cummings, P. Cherepanov, *Proc. Natl. Acad. Sci. USA* 107 (2010) 20057–20062.
- [21] Gaussian 09, Revision A.1, M.J. Frisch, G.W. Trucks, H.B. Schlegel, G.E. Scuseria, M.A. Robb, J.R. Cheeseman, G. Scalmani, V. Barone, B. Mennucci, G.A. Petersson, H. Nakatsuji, M. Caricato, X. Li, H.P. Hratchian, A.F. Izmaylov, J. Bloino, G. Zheng, J.L. Sonnenberg, M. Hada, M. Ehara, K. Toyota, R. Fukuda, J. Hasegawa, M. Ishida, T. Nakajima, Y. Honda, O. Kitao, H. Nakai, T. Vreven, J.A. Montgomery, Jr., J.E. Peralta, F. Ogliaro, M. Bearpark, J.J. Heyd, E. Brothers, K.N. Kudin, V.N. Staroverov, R. Kobayashi, J. Normand, K. Raghavachari, A. Rendell, J.C. Burant, S.S. Iyengar, J. Tomasi, M. Cossi, N. Rega, J.M. Millam, M. Klene, J.E. Knox, J.B. Cross, V. Bakken, C. Adamo, J. Jaramillo, R. Gomperts, R.E. Stratmann, O. Yazyev, A.J. Austin, R. Cammi, C. Pomelli, J.W. Ochterski, R.L. Martin, K. Morokuma, V.G. Zakrzewski, G.A. Voth, P. Salvador, J.J. Dannenberg, S. Dapprich, A.D. Daniels, O. Farkas, J.B. Foresman, J.V. Ortiz, J. Cioslowski, D.J. Fox, Gaussian Inc, Wallingford CT, 2009.
- [22] A.D. Becke, *J. Chem. Phys.* 98 (1993) 5648–5752.
- [23] C. Lee, W. Yang, R.G. Parr, *Phys. Rev. B* 37 (1988) 785–789.
- [24] CrysAlis RED, Oxford Diffraction Ltd., Version 1.171.29.2.
- [25] O.V. Dolomanov, L.J. Bourhis, R.J. Gildea, J.A.K. Howard, H. Puschmann, *J. Appl. Cryst.* 42 (2009) 229–341.
- [26] G.M. Sheldrick, *Acta Cryst. A* 64 (2008) 112–122.
- [27] M. Matsugi, F. Tabusa, J. Minamikawa, *Tetrahedron Lett.* 41 (2000) 8523–8525.
- [28] G.R. Desiraju, T. Steiner, *The Weak Hydrogen Bond in Structural Chemistry and Biology. IUCr Monograph on Crystallography*, vol. 9, Oxford University Press, 1999.
- [29] M.A. Spackman, D. Jayatilaka, *Cryst. Eng. Commun.* 11 (2009) 19–32.
- [30] M.A. Spackman, J.J. McKinnon, *Cryst. Eng. Commun.* 4 (2002) 378–392.
- [31] S.K. Wolff, D.J. Grimwood, J.J. McKinnon, M.J. Turner, D. Jayatilaka, M.A. Spackman, *CrystalExplorer (Version 3.1)*, University of Western Australia, 2012.
- [32] K. Uchiyama, A. Ono, Y. Hayashi, K. Narasaka, *Bull. Chem. Soc. Jpn.* 71 (1998) 2945–2955.
- [33] J.E. Nycz, G.J. Malecki, *J. Mol. Struct.* 1064 (2014) 44–49.